

# Solvothermal Synthesis and Characterization of Two Cd(II) Coordination Polymers with Isomeric Multi-carboxylate Ligands<sup>①</sup>

CAI Hua<sup>②</sup> LI Na LI Yan AN Dong-Min

(College of Science, Civil Aviation University of China, Tianjin 300300, China)

**ABSTRACT** In this work two isomeric semi-rigid multi-carboxylate ligands 3,5-bi(3-carboxyphenoxy)benzoic acid (3-H<sub>3</sub>BCP), 3,5-bi(4-carboxyphenoxy)benzoic acid (4-H<sub>3</sub>BCP) and two rigid ligands (bis-triazole 4-(4-(4H-1,2,4-triazol-4-yl)phenyl)-4H-1,2,4-triazole (L<sup>1</sup>), 2-(1H-pyrazol-3-yl)pyrazine (L<sup>2</sup>)) have been employed to react with Cd(II) salts under similar solvothermal reactions. Two novel Cd(II) mixed-ligand coordination polymers, namely, {[Cd<sub>3</sub>(3-BCP)<sub>2</sub>(L<sup>1</sup>)] 3H<sub>2</sub>O}<sub>n</sub> (**1**) and [Cd(4-HBCP)(L<sup>2</sup>)]<sub>n</sub> (**2**), have been isolated. **1** displays a rare 2D cluster-based network while **2** displays a 3D supramolecular network through weak interactions. Solid-state luminescent properties and thermal analyses of **1** and **2** also have been determined, indicating strong fluorescent emissions and good thermal stabilities. Different coordination modes of two semi-rigid multi-carboxylate ligands and L<sup>1</sup> and L<sup>2</sup> also have been briefly discussed, which also reveal the great potential in the construction of these novel mixed-ligand luminescent frameworks with diverse structural motifs and unique functional properties.

**Keywords:** isomeric, semirigid multicarboxylate, photoluminescent properties;

**DOI:** 10.14102/j.cnki.0254-5861.2011-2995

## 1 INTRODUCTION

Coordination polymers (CPs) in magnetics, sensors, gas adsorption, ion exchange, catalysis, and other fields have broad application prospects and become hot many laboratory studies in recent years<sup>[1-9]</sup>. An effective and facile method for the design of two-dimensional (2D) and three-dimensional (3D) metallosupramolecular species is still the appropriate choice of well-designed organic ligands as bridges or terminal groups (building blocks) with metal ions or metal clusters as nodes<sup>[10-12]</sup>. Among various organic ligands, semirigid multicarboxylate ligands with two or more aromatic rings separated by O atoms are often selected as multifunctional organic linkers because of their abundant coordination modes to metal ions, allowing for various structural topologies and because of their ability to act as H-bond acceptors and donors to assemble supramolecular structures. The conformational freedom nature of the flexible ligand may provide more possibility for the construction of unusual topology structures and microporous coordination polymers<sup>[13-17]</sup>. As we all know, the mixed ligand strategy has added the scope of the

functional CPs and given diverse polymeric structures with interesting structures and unusual properties<sup>[18-21]</sup>. Multidentate N-donor rigid ligands, such as 4,4'-bipyridine, bis-triazole 4-(4-(4H-1,2,4-triazol-4-yl)phenyl)-4H-1,2,4-triazole, and 2-(1H-pyrazol-3-yl)pyrazine<sup>[22-25]</sup>, have been employed as auxiliary ligands in the fabrication of CPs. Therefore, it is worth trying to prepare novel functional metal-organic hybrid complexes by using such kind of isomeric semirigid multicarboxylate and auxiliary bridging linkers.

The aforementioned points inspired us to assemble novel coordination frameworks with semirigid 3,5-bi(3-carboxyphenoxy) benzoic acid (3-H<sub>3</sub>BCP), 3,5-bi(4-carboxyphenoxy)benzoic acid (4-H<sub>3</sub>BCP) and auxiliary linkers bis-triazole 4-(4-(4H-1,2,4-triazol-4-yl)phenyl)-4H-1,2,4-triazole (L<sup>1</sup>) and 2-(1H-pyrazol-3-yl)pyrazine (L<sup>2</sup>). Herein, under similar solvothermal conditions, two novel mixed-ligand Cd(II) coordination polymers, namely, {[Cd<sub>3</sub>(3-BCP)<sub>2</sub>(L<sup>1</sup>)] 3H<sub>2</sub>O}<sub>n</sub> (**1**) and [Cd(4-HBCP)(L<sup>2</sup>)]<sub>n</sub> (**2**), have been isolated and investigated by elemental analysis, FT-IR, powder X-ray diffraction (PXRD) techniques, thermal analysis and fluorescence characterization.

Received 27 September 2020; accepted 5 January 2021 (CCDC 2034000 (**1**) and 2033999 (**2**))

① Scientific Research Project of Tianjin Education Commission (2018KJ250) and National Natural Science Foundation of China (21501196)

② Corresponding author. E-mail: caihua-1109@163.com

## 2 EXPERIMENTAL

### 2.1 General

All reagents and solvents for synthesis and analysis were commercially available and used as received. Fourier transform (FT) IR spectra (KBr pellets) were taken on an AVATAR-330 (Nicolet) spectrometer. Microanalyses of C, H, and N were carried out on a CE-440 (Leemanlabs) analyzer. Powder X-ray diffraction (PXRD) patterns were recorded on a Rigaku D/Max-2500 diffractometer at 40 kV and 100 mA for a Cu-target tube ( $\lambda = 1.5406 \text{ \AA}$ ). Thermogravimetric analysis (TGA) was carried out on a Dupont thermal analyzer from room temperature to 600 °C under N<sub>2</sub> atmosphere at a heating rate of 10 °C/min. Solid-state UV-Vis diffuse reflectance spectra were performed at room temperature using Shimadzu UV-3600 double monochromatic spectrophotometer with BaSO<sub>4</sub> as a 100% reflectance standard for all materials. Fluorescence spectra of the polycrystalline powder samples were performed on a HITACHI spectrofluorimeter (F7000) equipped with a xenon lamp and quartz carrier at room temperature.

### 2.2 Synthesis of the complexes

**Synthesis of 1** A mixture containing Cd(OAc)<sub>2</sub> · 2H<sub>2</sub>O (22 mg, 0.10 mmol), L<sup>1</sup> (21.2 mg, 0.10 mmol), 3-H<sub>3</sub>BCP (39.4 mg, 0.10 mmol) and (10 mL) was sealed in a Teflon-lined stainless-steel vessel (20 mL), which was heated at 140 °C for 3 days and then cooled to room temperature at a rate of 5 °C h<sup>-1</sup>. Colorless block crystals of **1** were obtained with 47% yield (18.4 mg, based on 3-H<sub>3</sub>BCP). Anal. Calcd. for C<sub>52</sub>H<sub>36</sub>Cd<sub>3</sub>N<sub>6</sub>O<sub>19</sub>: C, 45.06; H, 2.62; N, 6.06%. Found: C, 45.23; H, 2.66; N, 6.09%. IR (KBr, cm<sup>-1</sup>): 3637m, 3125b, 3110m, 1625s, 1544m, 1504m, 1380s, 1252s, 1210m, 1040w,

1010m, 1001w, 970m, 912w, 894w, 692m, 645m.

**Synthesis of 2** The same synthetic method as that for **1** was used except that 3-H<sub>3</sub>BCP and L<sup>1</sup> were replaced by 4-H<sub>3</sub>BCP (39.4 mg, 0.10 mmol) and L<sup>2</sup>, respectively. Colorless block crystals of **2** were obtained with 44% yield (15.6 mg, based on 4-H<sub>3</sub>BCP). Anal. Calcd. for C<sub>28</sub>H<sub>18</sub>CdN<sub>4</sub>O<sub>8</sub>: C, 51.67; H, 2.79; N, 8.61%. Found: C, 51.61; H, 2.73; N, 8.59%. IR (KBr, cm<sup>-1</sup>): 3416m, 1662m, 1534m, 1415m, 1398s, 1259w, 1216m, 1151w, 1085w, 991m, 865m, 842m, 809m, 758m, 708w, 643w.

### 2.3 Structure determination

Single-crystal X-ray diffraction data for complexes **1** (0.36mm × 0.28mm × 0.20mm) and **2** (0.28mm × 0.22mm × 0.20mm) were collected on a Bruker Apex II CCD diffractometer at 293(2) K with MoK $\alpha$  radiation ( $\lambda = 0.071073 \text{ nm}$ ). There was no evidence of crystal decay during data collection. In general, a semi-empirical absorption correction (SADABS) was applied, and the program SAINT was used for the integration of the diffraction profiles<sup>[22]</sup>. The structures were solved by direct methods using the SHELXS program of the SHELXTL package and refined with SHELXL<sup>[23]</sup>. The final refinement was performed by full-matrix least-squares methods on  $F^2$  with anisotropic thermal parameters for all non-H atoms. Hydrogen atoms attached to carbon were generated geometrically and those of methanol or water were first located in difference Fourier syntheses and then treated as riding. Isotropic displacement parameters of H were derived from their parent atoms. A summary of the crystallographic data is shown in Table 1. Selected bond parameters are listed in Table 2, and hydrogen bonds are listed in Table 3.

Table 1. Crystal Data of Complexes 1 and 2

Complex	1	2	Complex	1	2
Chemical formula	C <sub>52</sub> H <sub>36</sub> Cd <sub>3</sub> N <sub>6</sub> O <sub>19</sub>	C <sub>28</sub> H <sub>18</sub> CdN <sub>4</sub> O <sub>8</sub>	$F(000)$	1372	652
Formula mass	1386.07	650.86	$Z$	2	2
Crystal system	Triclinic	Triclinic	Absorption coefficient ( $\mu/\text{mm}^{-1}$ )	1.312	0.900
Space group	$P\bar{1}$	$P\bar{1}$	No. of reflections measured	14764	7386
$a$ (Å)	12.174(3)	10.369(9)	No. of independent reflections	9969	5017
$b$ (Å)	14.144(4)	11.189(10)	$R_{\text{int}}$	0.024	0.0204
$c$ (Å)	16.441(5)	12.847(11)	Final $R$ values ( $I > 2\sigma(I)$ )	0.0402	0.0311
$\alpha$ (°)	75.732(4)	95.543(12)	Final $wR$ ( $F^2$ ) values ( $I > 2\sigma(I)$ )	0.0799	0.0691
$\beta$ (°)	83.322(4)	96.844(13)	Final $R$ values (all data)	0.0689	0.0378
$\gamma$ (°)	69.936(3)	116.884(10)	Final $wR$ ( $F^2$ ) values (all data)	0.0917	0.0732
Volume (Å <sup>3</sup> )	2575.7(12)	1301(2)	Goodness of fit on $F^2$	1.013	1.031
Temperature (K)	296(2)	296(2)	Residuals ( $e/\text{\AA}^3$ )	0.693, -0.599	0.828, -0.417

Table 2. Selected Bond Lengths (Å) and Bond Angles (°) for Complexes 1 and 2

Bond	Dist.	Bond	Dist.	Bond	Dist.
<b>1</b>					
Cd(1)–O(2)a	2.208(3)	Cd(1)–O(13)b	2.298(3)	Cd(1)–N(1)	2.326(3)
Cd(1)–O(12)b	2.333(3)	Cd(1)–O(4)	2.371(3)	Cd(1)–O(5)	2.415(3)
Cd(2)–O(1)a	2.236(4)	Cd(2)–O(9)	2.248(4)	Cd(2)–N(2)	2.274(4)
Cd(2)–O(8)c	2.291(3)	Cd(2)–N(6)d	2.296(4)	Cd(2)–O(5)	2.369(3)
Cd(3)–O(10)	2.185(4)	Cd(3)–O(16)e	2.236(4)	Cd(3)–O(7)c	2.312(3)
Cd(3)–N(5)d	2.399(3)	Cd(3)–O(8)c	2.427(3)	Cd(3)–O(15)e	2.493(4)
<b>2</b>					
Cd(1)–N(3)	2.301(3)	Cd(1)–O(1)	2.323(3)	Cd(1)–O(5)f	2.369(2)
Cd(1)–O(2)	2.380(2)	Cd(1)–O(2)g	2.412(3)	Cd(1)–O(4)f	2.449(3)
Cd(1)–N(1)	2.469(3)				
Angle (°)		Angle (°)		Angle (°)	
<b>1</b>					
O(2)a–Cd(1)–O(13)b	145.26(14)	O(2)a–Cd(1)–N(1)	100.34(13)	O(2)a–Cd(1)–O(4)	92.62(13)
O(13)b–Cd(1)–N(1)	81.79(12)	O(2)a–Cd(1)–O(12)b	95.56(13)	N(1)–Cd(1)–O(4)	136.89(13)
O(13)b–Cd(1)–O(12)b	56.68(12)	N(1)–Cd(1)–O(12)b	122.56(12)	O(2)a–Cd(1)–O(5)	110.49(12)
O(13)b–Cd(1)–O(4)	109.56(13)	N(1)–Cd(1)–O(5)	82.33(12)	O(12)b–Cd(1)–O(5)	140.54(12)
O(12)b–Cd(1)–O(4)	96.44(12)	O(4)–Cd(1)–O(5)	54.69(10)	O(1)a–Cd(2)–O(9)	103.99(15)
O(13)b–Cd(1)–O(5)	104.18(12)	O(1)a–Cd(2)–N(2)	92.81(15)	O(9)–Cd(2)–N(2)	92.99(13)
O(1)a–Cd(2)–O(8)c	164.44(14)	O(9)–Cd(2)–O(8)c	88.06(14)	O(8)c–Cd(2)–N(6)d	82.96(13)
N(2)–Cd(2)–O(8)c	96.40(13)	O(1)a–Cd(2)–N(6)d	87.51(14)	O(9)–Cd(2)–O(5)	171.86(13)
O(9)–Cd(2)–N(6)d	88.38(13)	N(2)–Cd(2)–N(6)d	178.47(14)	O(8)c–Cd(2)–O(5)	83.84(12)
O(1)a–Cd(2)–O(5)	84.12(14)	N(2)–Cd(2)–O(5)	87.11(12)	N(6)d–Cd(2)–O(5)	91.43(12)
O(10)–Cd(3)–O(16)e	123.92(15)	O(10)–Cd(3)–O(7)c	95.40(17)	O(7)c–Cd(3)–O(8)c	54.37(11)
O(16)e–Cd(3)–O(7)c	122.62(16)	O(10)–Cd(3)–N(5)d	110.56(15)	O(10)–Cd(3)–O(15)e	90.99(16)
O(16)e–Cd(3)–N(5)d	78.66(14)	O(7)c–Cd(3)–N(5)d	128.18(13)	O(7)c–Cd(3)–O(15)e	89.48(15)
O(10)–Cd(3)–O(8)c	102.95(14)	O(16)e–Cd(3)–O(8)c	132.10(14)	O(8)c–Cd(3)–O(15)e	141.87(15)
N(5)d–Cd(3)–O(8)c	75.98(11)	O(16)e–Cd(3)–O(15)e	54.24(14)	N(5)d–Cd(3)–O(15)e	131.96(14)
<b>2</b>					
N(3)–Cd(1)–O(1)	111.62(9)	N(3)–Cd(1)–O(5)f	117.01(8)	O(1)–Cd(1)–O(5)f	122.03(10)
N(3)–Cd(1)–O(2)	103.03(8)	O(1)–Cd(1)–O(2)	55.61(8)	O(5)f–Cd(1)–O(2)	133.04(8)
N(3)–Cd(1)–O(2)g	80.90(8)	O(1)–Cd(1)–O(2)g	130.37(7)	O(5)f–Cd(1)–O(2)g	87.67(10)
O(2)–Cd(1)–O(2)g	74.91(10)	N(3)–Cd(1)–O(4)f	159.85(9)	O(1)–Cd(1)–O(4)f	86.79(9)
O(5)f–Cd(1)–O(4)f	53.85(7)	O(2)–Cd(1)–O(4)f	80.15(8)	O(2)g–Cd(1)–O(4)f	80.78(8)
N(3)–Cd(1)–N(1)	68.17(10)	O(1)–Cd(1)–N(1)	93.19(8)	O(5)f–Cd(1)–N(1)	77.93(9)
O(2)–Cd(1)–N(1)	143.22(9)	O(2)g–Cd(1)–N(1)	134.13(9)	O(4)g–Cd(1)–N(1)	120.79(8)

Symmetry transformation: a:  $-x, -y, -z+2$ ; b:  $-x, -y+1, -z+2$ ; c:  $-x, -y+1, -z+1$ ; d:  $x, y-1, z$ ; e:  $x, y, z-1$ ; f:  $-x+1, -y+2, -z$ ; g:  $-x, -y+2, -z$ 

Table 3. Hydrogen Bond Lengths (Å) and Bond Angles (°) for Complex 2

D–H...A	d(D–H)	d(H...A)	d(D...A)	∠DHA
N(4)–H(4A)...O(4) <sup>a</sup>	0.86	1.92	2.749(4)	162
O(8)–H(8)...O(6) <sup>b</sup>	0.82	1.84	2.654(4)	171

Symmetry codes: a:  $x-1, y, z$ ; b:  $-x+2, -y+1, -z+1$ 

### 3 RESULTS AND DISCUSSION

#### 3.1 Crystal structure description

Complex **1** represents a 2D coordination array with trinuclear Cd(II) subunits. The asymmetric unit is composed of three Cd(II) atoms, a  $L^1$  ligand, a pair of 3-BCP<sup>3-</sup> ligands, and three lattice water molecules (Fig. 1a). Interestingly, both Cd(II) ions have different coordination spheres (see Table 2

for detailed bond parameters). The Cd(1) is coordinated by three 3-BCP<sup>3-</sup> ligands and one  $L^1$  ligand. The resulting CdNO<sub>5</sub> octahedral core shows considerable distortion. The Cd–O bond lengths are in the range of 2.208(3)~2.415(3) Å and the Cd–N bond distances are 2.326(3) Å. Although Cd(2) binds to four oxygen atoms from three 3-BCP<sup>3-</sup> ligands and two nitrogen atoms from  $L^1$  ligands, it also shows a distorted octahedral geometry (CdN<sub>2</sub>O<sub>4</sub>) with the N(2)–Cd(2)–N(6)

angle of  $178.47(14)^\circ$ . The coordination sphere of Cd(3) atom is six-coordinated ( $O_5N$ ) and resides in a distorted octahedral coordination environment. The square base of Cd(3) is nonplanar and occupied by O(7), O(10), O(16) and N(5) from three 3-BCP<sup>3-</sup> ligands and one L<sup>1</sup> ligand. The axial positions of Cd(3) are coordinated by O(8) and O(15) from 3-BCP<sup>3-</sup> ligand. The Cd–O bond lengths fall in the range of  $2.185(4) \sim 2.493(4)$  Å and the Cd–N bond distances are  $2.399(3)$  Å<sup>[24]</sup>. Thus, three Cd(II) centers are linked by two 3-BCP<sup>3-</sup> and one L<sup>1</sup> to result in a trinuclear unit with the Cd(1)⋯Cd(2) and Cd(2)⋯Cd(3) separation of  $3.6498(3)$  and  $3.7271(11)$  Å. Such

a pattern is unknown in metal coordination, as suggested by a Cambridge Structural Database (CSD) search (version 5.37, Feb 2018). These subunits are extended into a 2D layer, which is decorated by the 3-BCP<sup>3-</sup> ligands as dangling arms (Fig. 1b). Topologically, **1** can be rationalized to a novel (4,4,4,4,6,6)-connected 6-nodal topological network, Point symbol  $(4^2.6^2.8^2)(4^2.6^3.8)(4^4.6^2)_2(4^7.6^7.8)(4^9.6^6)$  by denoting L<sup>1</sup> to the 4-connected nodes, and Scheme 1a 3-BCP<sup>3-</sup> ligand, and Scheme 1b 3-BCP<sup>3-</sup> ligand to 6-, and 4-connected nodes, respectively (Fig. 1c).

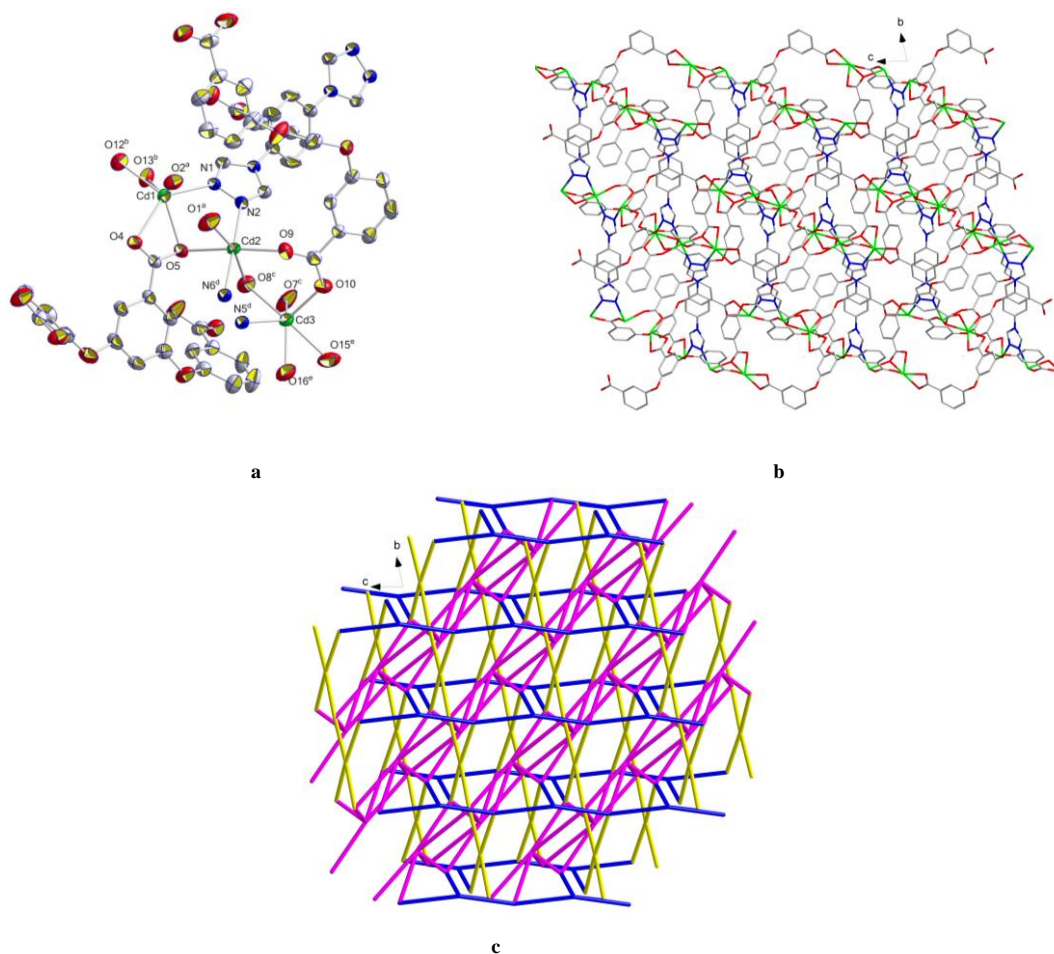


**Fig. 1.** Crystal structure of **1**. (a) Coordination environment of Cd(II) in **1** (symmetry codes: a =  $-x, -y, -z + 2$ ; b =  $-x, -y + 1, -z + 2$ ; c =  $-x, -y + 1, -z + 1$ ; d =  $x, y - 1, z$ ; e =  $x, y, z - 1$ ). (b) Perspective view of the 2D layer. (c) View of the topological structure of the 2D network of **1**

Complex **2** has a centrosymmetric dinuclear structure (Fig. 2a) with the Cd(II) ion seven-coordinated by two N atoms from one chelating L<sup>2</sup> ligand and five O atoms from three 4-HBCP<sup>2-</sup> ligands. L<sup>2</sup> acts as a typical chelating ligand coordinating to the Cd(II) ion with the Cd–N bond distances ranging from  $2.301(3)$  to  $2.469(3)$  Å and the N–Cd–N angle being  $68.17(10)^\circ$ . For 4-HBCP<sup>2-</sup>, carboxyl groups exhibit two

different coordination modes with Cd(II) ion; namely, one (O(4), O(5)) chelates with Cd(1) bidentately, while the other (O(1), O(2)) adopts a  $\mu_3$  chelating-bridging coordination mode to connect two Cd(II) ions (i.e., Cd(1) and Cd(1A)) to form a dinuclear structure (The Cd(1)⋯Cd(1A) distance is  $3.804(3)$  Å). The 4-HBCP<sup>2-</sup> anion acts as a bis-tridentate ligand to bridge the two coplanar Cd(II) ions, resulting in a

1D double-chain structure. The Cd(1)–O ones extend from 2.323(3) to 2.449(3) Å. The Cd(1)–O(1) bond distance (2.449(3) Å) is longer than Cd(1)–O(2) (2.323(3) Å), suggesting that carboxylic group coordination modes are asymmetric, and this is common in  $\mu_3$  carboxylic metal coordination. Also, all these Cd–N, Cd–O bond distances and the bond angles around each Cd(II) center are in the normal

ranges expected for such coordination complexes (Table 2)<sup>[24]</sup>. It is worth noting that the N(4) atom of  $L^2$  is not coordinated to Cd(II) ions, which presents strong intermolecular hydrogen-bonding interactions with coordinated O(4A) atom of 4-HBCP<sup>2-</sup> ligand (N(4)···O(4A) separation 2.749(4) Å, N(4)–H(4A)···O(4A) angle 162°, symmetry code a:  $x-1, y, z$ ) (Table 3), which further stabilizes the 1D structure (Fig. 2b).

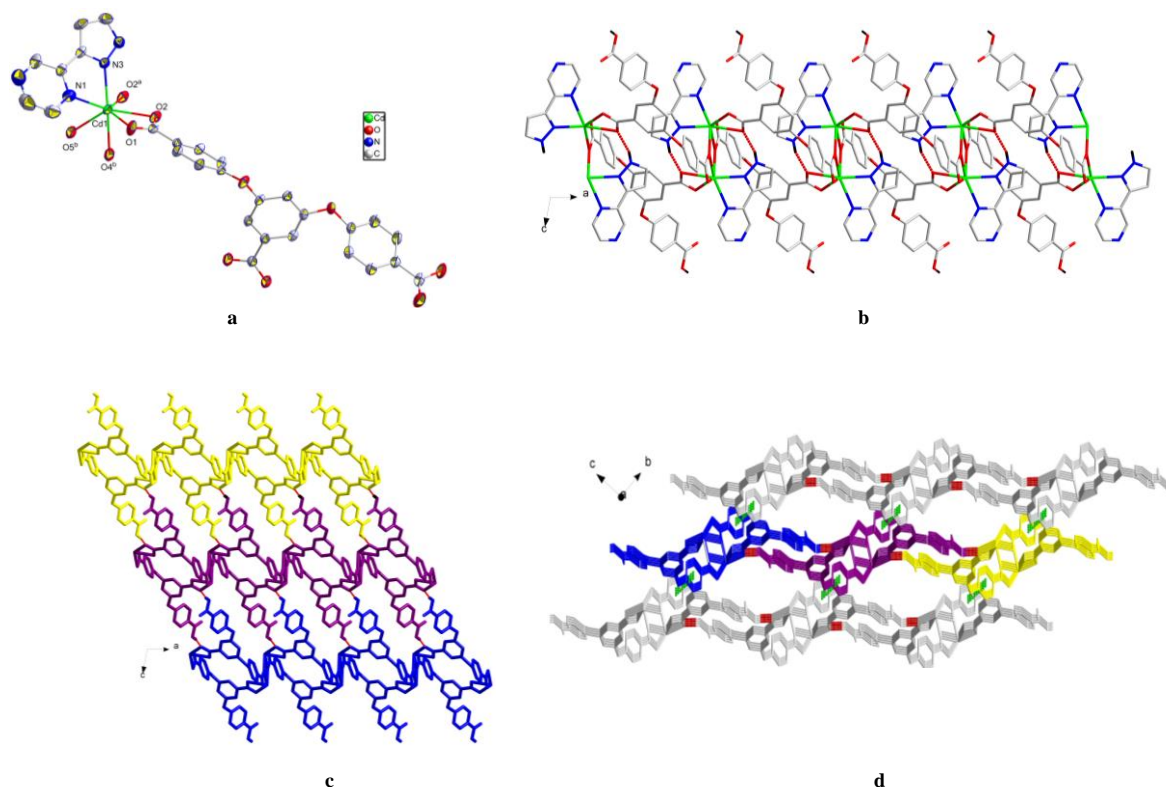
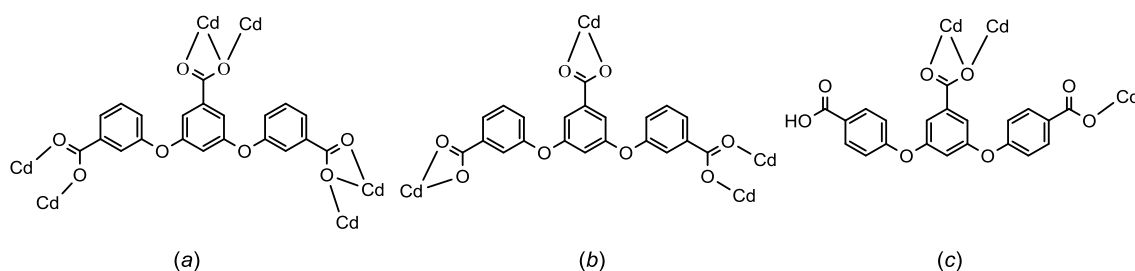


**Fig. 2.** Crystal structure of **2**. (a) Coordination environment of Cd(II) in **2** (symmetry codes: a =  $-x, -y + 2, -z$ , b =  $-x + 1, -y + 2, -z$ ). (b) A perspective view of the 1D double chain. (c) A perspective view of the 2D supramolecular network of **2** with O–H···O hydrogen bonds ( $L^2$  are omitted for clarity). (d) 3D supramolecular framework of complex **2** formed through aromatic stacking ( $L^2$  are omitted for clarity)

Besides, the adjacent discrete 1D chains are arranged into a 2D supramolecular layer by intermolecular O–H···O hydrogen bonding. The O(8)···O(5) separation is 2.654(4) Å with the O(8)–H(8)···O(5) angle of 171° (symmetry code b:  $-x+2, -y+1, -z+1$ , see also Table 3) (Fig. 2c). Additionally, the adjacent 2D supramolecular layers show  $\pi$ – $\pi$  stacking interactions between phenyl-phenyl rings from adjacent 4-HBCP<sup>2-</sup> ligands with the centroid-centroid separation of 3.495(4) Å, which ultimately forms a 3D supramolecular structure (Fig. 2d).

It is noteworthy that dramatic structural differences are observed in polymers **1** and **2**, based on the selection of

semirigid tricarboxylate ligands with three different coordination modes as building blocks. These tectons show different binding fashions as illustrated in Scheme 1. For **1**, 3-BCP<sup>3-</sup> ligands adopt two different coordination modes. One is bidentate bridging and chelating bidentate bridge, and the other is the chelating bridging anions, as observed in **1**, where the  $\mu_6$ -3-BCP<sup>3-</sup> (Scheme 1a) and  $\mu_4$ -3-BCP<sup>3-</sup> (Scheme 1b) anions afford the 2D layer array. However, the monodentate and chelating bidentate bridging anions are found in **2**, and the Cd(II) metal centers are extended by  $\mu_3$ -4-HBCP<sup>2-</sup> (Scheme 1c) linkers to result in a 1D double chain.



Scheme 1. Different coordination modes for two isomeric multicarboxylates 3-H<sub>3</sub>BCP and 4-H<sub>3</sub>BCP

### 3. 2 FT-IR, PXRD, TGA and fluorescence property studies

In the FT-IR spectra of complex **1**, there are 3211 and 3175  $\text{cm}^{-1}$  medium bands around 3000~3250  $\text{cm}^{-1}$ , showing the existence of lattice water molecules in the coordination framework and the asymmetric and symmetric stretching vibrations of carboxylate groups are observed in the ranges of 1510 ~ 1542 and 1320 ~ 1434  $\text{cm}^{-1}$ , respectively, which indicate complete deprotonation of the carboxylic groups in **1**<sup>[25]</sup>. In the same spectra for **2**, broad bands are found around 3250~3650  $\text{cm}^{-1}$ , which suggests the existence of O–H and

N–H in the coordination framework. The bands around 1600  $\text{cm}^{-1}$  indicate incomplete deprotonation of the carboxylic groups. All are in agreement with the X-ray single-crystal analysis results.

For complexes **1** and **2**, PXRD analyses were performed at room temperature, taking the powder samples of each complex to confirm the phase purity of the bulk materials. In all complexes there is a good agreement of the entire peak positions between the experimental and simulated PXRD patterns from their corresponding single crystal structures (see Fig. 3 (a) and (b) for PXRD patterns).

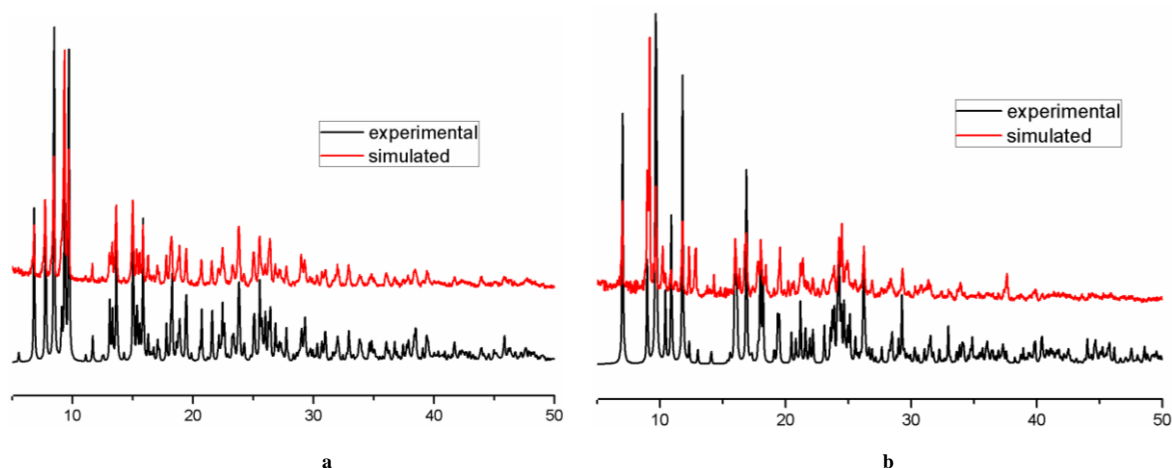


Fig. 3. (a) PXRD pattern of simulated (red) and experimental (black) of complex **1**;  
(b) PXRD pattern of simulated (red) and experimental (black) of complex **2**

There was no evidence of crystal decay during X-ray data collection for **1** and **2** which are stable at ambient conditions. Thus, thermogravimetric analysis (TGA) experiments of these Cd(II) coordination polymers have been performed to explore their thermal stabilities (Fig. 4). For **1**, the first weight loss of 4.1% between 50 and 305 °C corresponds to the departure of three lattice water molecules (calculated, 3.9%), and then the network is quickly decomposed until 700 °C. Complex **2** is thermally stable upon heating to 319 °C followed by a sharp weight loss ending at 401 °C and a slow weight loss not ending until 700 °C. It is noted that a continuous mass loss

after 400 °C can be observed for **1** and **2**, and no obvious platform can be observed. The result reveals these coordination polymers should be completely decomposed above 400 °C.

Coordination polymers with conjugated organic ligands have good thermal stability and controllable photoluminescence, so they are ideal materials for the preparation of photoactive materials. Therefore, solid state fluorescence properties of polymeric Cd(II) complexes (with  $d^{10}$  electron configuration) were studied at room temperature. As shown in Fig. 5 (a) and (b), at ambient temperature, the free ligands L<sup>1</sup>,

$L^2$ , 3- $H_3BCP$  and 4- $H_3BCP$  in the solid state are luminescent and show the broad emission maximum at 318, 354, 344 and 352 nm, respectively ( $\lambda_{ex} = 279$  nm for  $L^1$ ,  $\lambda_{ex} = 330$  nm for 3- $H_3BCP$  and 4- $H_3BCP$ ,  $\lambda_{ex} = 320$  nm for  $L^2$ ). For these ligands, the chromophores are the aromatic rings and the observed emission is due to the  $\pi-\pi^*$  transition. Solid-state fluorescence spectra of **1** and **2** at room temperature have been

determined. In comparison with that of free ligand  $L^1$ ,  $L^2$ , 3- $H_3BCP$  and 4- $H_3BCP$ , **1** and **2** show strong emission bands centered at 395 and 441 nm ( $\lambda_{ex} = 320$  nm), respectively, which is different from that of  $L^1$ ,  $L^2$ , 3- $H_3BCP$  and 4- $H_3BCP$  ascribed to the ligand-to-metal charge-transfer (LMCT) bands<sup>[26]</sup>.

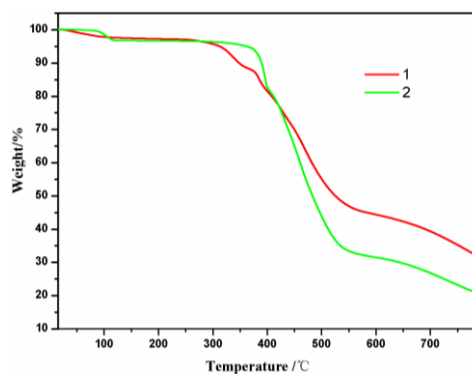


Fig. 4. Thermogravimetric analysis (TGA) curves of complexes **1** and **2**

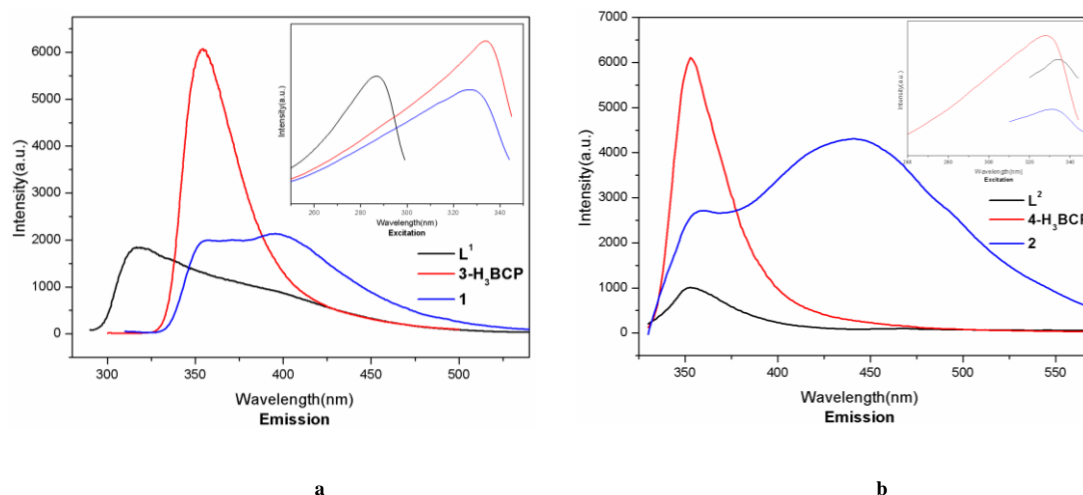


Fig. 5. (a) Solid-state fluorescent emissions and excitations at room temperature of complex **1**;  
(b) Solid-state fluorescent emissions and excitations at room temperature of complex **2**

### 3.3 UV-Vis absorption spectrum

The UV-Vis absorption spectra of complexes **1** and **2** show intense wide absorption peaks at 220~350 nm for **1** and **2**, which can be assigned as ligand-to-metal charge-transfer (LMCT) transitions<sup>[27, 28]</sup>, while lower energy bands (270~300 nm for **1**, 250~300 nm for **2**) are assigned as the  $\pi \rightarrow \pi^*$  electron transition between ligands (Fig. 6).

## 4 CONCLUSION

In summary, two rigid ligands 4-(4-(4H-1,2,4-triazol-4-yl)phenyl)-4H-1,2,4-triazole ( $L^1$ ), 2-(1H-pyrazol-3-yl)pyrazine ( $L^2$ ) and two isomeric semi-rigid 3,5-bi(3-carboxy-

phenoxy)benzoic acid (3- $H_3BCP$ ) and 3,5-bi(4-carboxyphenoxy)benzoic acid (4- $H_3BCP$ ) have been employed, and two distinct mixed-ligand luminescent coordination polymers  $\{[Cd_3(3-BCP)_2(L^1)] \cdot 3H_2O\}_n$  (**1**) and  $[Cd(4-HBCP)(L^2)]_n$  (**2**) have been isolated. **1** exhibits unusual network topology with point symbol  $(4^2.6^2.8^2)(4^2.6^3.8)(4^4.6^2)_2(4^7.6^7.8)(4^9.6^6)$ . Both **1** and **2** have high thermal stabilities and strong fluorescent emissions. This work clearly demonstrates that various isomeric semirigid aromatic poly-carboxylate ligands can be applied as versatile building blocks to construct these coordination polymers with interesting network structures and unique functional properties.



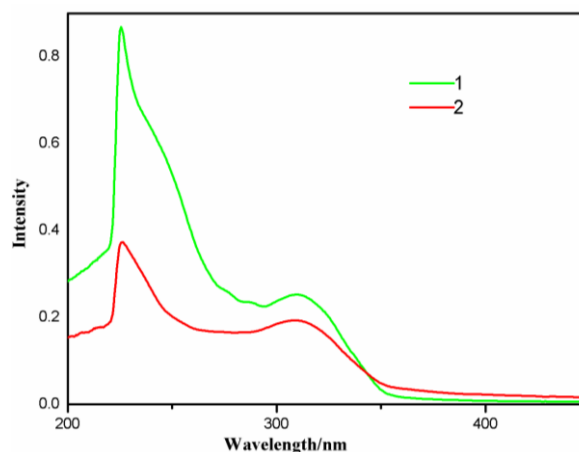


Fig. 6. UV-Vis absorption spectra of complexes 1 and 2

## REFERENCES

- (1) Dau, P. V.; Cohen, S. M. Cyclometalated metal-organic frameworks as stable and reusable heterogeneous catalysts for allylic N-alkylation of amines. *Chem. Commun.* **2013**, 49, 6128–6130.
- (2) Férey, G.; Serre, C. Large breathing effects in three-dimensional porous hybrid matter: facts, analyses, rules and consequences. *Chem. Soc. Rev.* **2009**, 38, 1380–1399.
- (3) He, H. M.; Zhu, Q. Q.; Li, C. P.; Du, M. Design of a highly-stable pillar-layer zinc(II) porous framework for rapid, reversible, and multi-responsive luminescent sensor in water. *Cryst. Growth Des.* **2019**, 19, 694–703.
- (4) Gu, J. Z.; Wen, M.; Cai, Y.; Shi, Z. F.; Nesterov, D. S.; Kirillova, M. V.; Kirillov, A. M. Metal-organic architectures assembled from multifunctional polycarboxylates: hydrothermal self-assembly, structures, and catalytic activity in alkane oxidation. *Inorg. Chem.* **2019**, 58, 2403–2412.
- (5) Liu, H.; Kang, Y. F.; Fan, Y. P.; Guo, F. S.; Liu, L.; Li, J. L.; Liu, P.; Wang, Y. Y. Highly thermally and chemically stable nickel(II) coordination polymers: tentative studies on their synthesis, catalysis, and magnetism. *Cryst. Growth Des.* **2019**, 19, 797–807.
- (6) Zou, J. Y.; Shi, W.; Gao, H. L.; Cui, J. Z.; Cheng, P. Spin canting and metamagnetism in 3D pillared-layer homospin cobalt(II) molecular magnetic materials constructed via a mixed ligands approach. *Inorg. Chem. Front.* **2014**, 1, 242–248.
- (7) Ding, B.; Ma, D. X.; Zhang, H. M.; Meng, X.; Qiu, R. R.; Ren, R.; Wu, J.; Wu, X. X.; Huo, J. Z.; Liu, Y. Y.; Shi, X. F. Solvo-thermal synthesis of a unique alkaline earth-transition Ba-Cd micro-porous coordination framework as hetero-metallic luminescent sensor for Cu<sup>2+</sup> and real-time detection of benzaldehyde. *Spectrochim. Acta, Part A* **2018**, 199, 110–116.
- (8) Liu, Y. H.; Zhang, F. J.; Wu, P. Y.; Deng, C. F.; Yang, Q. M.; Xue, J. J.; Shi, Y. H.; Wang, J. Cobalt(II)-based metal-organic framework as bifunctional materials for Ag(I) detection and proton reduction catalysis for hydrogen production. *Inorg. Chem.* **2019**, 58, 924–931.
- (9) Chen, M.; Zhao, H.; Liu, C. S.; Wang, X.; Shi, H. Z.; Du, M. Template-directed construction of conformational supramolecular isomers for bilayer porous metal-organic frameworks with distinct gas sorption behaviors. *Chem. Commun.* **2015**, 51, 6014–6017.
- (10) Mondal, P.; Dey, B.; Roy, S.; Bera, S. P.; Nasani, R.; Santra, A.; Konar, S. Field-induced slow magnetic relaxation and anion/solvent dependent proton conduction in cobalt(II) coordination polymers. *Cryst. Growth Des.* **2018**, 18, 6211–6220.
- (11) Wang, Y.; Lin, H. X.; Chen, L.; Ding, S. Y.; Lei, Z. C.; Liu, D. Y.; Cao, X. Y.; Liang, H. J.; Jiang, Y. B.; Tian, Z. Q. What molecular assembly can learn from catalytic chemistry? *Chem. Soc. Rev.* **2014**, 43, 399–411.
- (12) Ardila-Suárez, C.; Díaz-Lasprilla, A. M.; Díaz-Vaca, L. A.; Balbuena, P. B.; Baldovino-Medrano, V. G.; Ramírez-Caballero, G. E. Synthesis, characterization, and post-synthetic modification of a micro/mesoporous zirconium-tricarboxylate metal-organic framework: towards the addition of acid active sites. *CrystEngComm.* **2019**, 21, 3014–3030.
- (13) Ma, Y. M.; Liu, T.; Huang, W. H. Synthesis of a 3D lanthanum(III) MOFs as a multi-chemosensor to Cr(VI)-containing anion and Fe(III) cation based on a flexible ligand. *J. Solid State Chem.* **2018**, 258, 176–180.
- (14) Wang, Z. W.; Chen, M.; Liu, C. S.; Wang, X.; Zhao, H.; Du, M. A versatile Al<sup>III</sup>-based metal-organic framework with high physicochemical stability. *Chem. Eur. J.* **2015**, 21, 17215–17219.
- (15) Sun, Y. C.; Li, Z.; Liang, L. L.; Zhao, J. S.; Wang, J. L. Four transition metal coordination polymers based on an aromatic multi-carboxylic acid as



- ligand: syntheses, crystal structures, and fluorescent/magnetic properties. *Z. Anorg. Allg. Chem.* **2015**, 641, 953–961.
- (16) Fan, L. M.; Fan, W. L.; Song, W. K.; Sun, L. M.; Zhao, X.; Zhang, X. T. Structural diversity and magnetic properties of six metal-organic polymers based on semirigid tricarboxylate ligand of 3,5-bis(4-carboxyphenoxy)benzoic acid. *Dalton Trans.* **2014**, 43, 15979–15989.
- (17) Huang, W. H.; Li, J. Z.; Gao, L. S.; Wang, Y. X.; Liu, S. Y.; Jiang, M.; Liu, T.; Wang, Y. Y. The influence of structural isomerism on fluorescence and organic dye selective adsorption in two complexes based on flexible ligands. *Dalton Trans.* **2016**, 45, 15060–15066.
- (18) Qiu, Y. C.; Yuan, S.; Li, X. X.; Du, D. Y.; Wang, C.; Qin, J. S.; Drake, H. F.; Lan, Y. Q.; Jiang, L.; Zhou, H. C. Face-sharing archimedean solids stacking for the construction of mixed-ligand metal-organic frameworks. *J. Am. Chem. Soc.* **2019**, 141, 13841–13848.
- (19) Wang, Y. F.; He, C. J. Syntheses, crystal structures and characterization of two coordination polymers based on mixed ligands. *Chin. J. Struct. Chem.* **2018**, 37, 481–489.
- (20) Haque, F.; Halder, A.; Ghosh, S.; Maiti, A.; Ghoshal, D. Co-ligand-rigidity induced interpenetration in flexible bis-imidazolyl type linker based mixed ligand metal-organic frameworks. *Cryst. Growth Des.* **2019**, 19, 5152–5160.
- (21) Sun, Y.; Ma, R.; Wang, F.; Guo, X.; Sun, S.; Guo, H.; Alexandrov, E. V. Two novel self-catenated metal-organic frameworks with large accessible channels obtained by mixed-ligand strategy: adsorption of dichromate and  $\text{Ln}^{3+}$ -post synthetic modification. *Cryst. Growth Des.* **2019**, 19, 5267–5274.
- (22) Bruker AXS. SAINT Software Reference Manual, Madison, WI **1998**.
- (23) Sheldrick, G. M. *SHELXTL NT Version 5.1. Program for Solution and Refinement of Crystal Structures*. University of Göttingen, Germany **1997**.
- (24) Cui, J.; Yang, Q.; Li, Y.; Guo, Z.; Zheng, H. Syntheses, structures, photochemical and magnetic properties of novel divalent Cd/Mn coordination polymers based on a semirigid tripodal carboxylate ligand. *Cryst. Growth Des.* **2013**, 13, 1694–1702.
- (25) Nakamoto, K. *Infrared and Raman Spectra of Inorganic and Coordination Compounds*. John Wiley & Sons, New York **1986**.
- (26) Mahapatra, A. K.; Hazra, G.; Roy, J.; Sahoo, P. A simple coumarin-based colorimetric and ratiometric chemosensor for acetate and a selective fluorescence turn-on probe for iodide. *J. Lumines.* **2011**, 131, 1255–1259.
- (27) Guldi, D. M.; Mody, T. D.; Gerasimchuk, N. N.; Magda, D.; Sessler, J. L. Influence of large metal cations on the photophysical properties of texaphyrin, a rigid aromatic chromophore. *J. Am. Chem. Soc.* **2000**, 122, 8289–8298.
- (28) Jeremić, D. A.; Kaluderović, G. N.; Gámez-Ruiz, S.; Brčeski, I.; Kasalica, B.; Leovac, V. M. Large single crystals of isomorphous hexaaquametal(II) *d*-camphor-10-sulfonates. *Cryst. Growth Des.* **2010**, 10, 559–563.